BJC reports www.nature.com/bjcreports

ARTICLE OPEN

Check for updates

Small extracellular vesicles as biomarkers of response in recurrent/metastatic HNSCC patients treated with immunotherapy

Dan P. Zandberg[1], Chang-Sook Hong[1,2], Andrew Swartz[1], Ronan Hsieh[1], Jennifer Anderson[1], Robert L. Ferris[1], Brenda Diergaarde[1,3]✉ and Theresa L. Whiteside[1,4]✉

BACKGROUND: Biomarkers that effectively predict response to anti-PD-1 mAb therapy in cancer patients are an unmet need. We evaluated the utility of small extracellular vesicles (sEV) as biomarkers of response to immunotherapy in recurrent/metastatic (R/M) head and neck squamous cell carcinoma (HNSCC) patients.

METHODS: Plasma sEV were isolated from 24 R/M HNSCC patients prior to immunotherapy initiation. sEV were separated by immune capture into T cell-derived CD3(+) and tumor-enriched CD3(−) subsets. Stimulatory and suppressive profiles of CD3(−) sEV were determined by on-bead flow cytometry. Differences were assessed using nonparametric tests. Multivariable Cox regression was used to evaluate the relationship with overall (OS) and progression free survival (PFS).

RESULTS: CD3(−)CD44v3(+) sEV represented the majority of plasma sEV; the T-cell-derived CD3(+) fraction was significantly smaller. High CD3(+) sEV was associated with better OS and PFS. Total CD3(−)CD44v3(+) sEV was not associated with outcome. However, suppressive and stimulatory profiles were associated with OS; the suppressive/stimulatory ratio was associated with best response. Exploration of individual proteins on CD3(−) sEV showed that high PD-L1 and high CTLA-4 were associated with better outcomes.

CONCLUSIONS: Evaluation of the T cell-derived-CD3(+) and tumor-enriched CD3(−) plasma sEV subsets indicated their potential utility as biomarkers of response to immunotherapy.

BJC Reports; https://doi.org/10.1038/s44276-024-00096-0

INTRODUCTION

Squamous cell carcinoma of the head and neck (HNSCC) is the 6th most common malignancy worldwide and accounts for approximately 70,000 new cases and 16,000 deaths per year in the United States [1]. The most common primary sites are the oral cavity, oropharynx, larynx and hypopharynx [2]. Established risk factors include tobacco and alcohol use, and human papilloma virus (HPV) infection specifically for oropharyngeal cancer [2]. For patients with recurrent and/or metastatic HNSCC (R/M HNSCC), outcomes with systemic therapy alone remain poor [3]. Progress has been made in the last decade with the approval of nivolumab and pembrolizumab after failure of platinum-based chemotherapy in 2016, and more recently with the approval of pembrolizumab monotherapy or chemotherapy plus pembrolizumab in the first line setting in 2019 [4]. Like other solid tumors, prolonged duration of response to anti-PD-1 monoclonal antibody (mAb) therapy has driven an overall survival benefit compared to standard chemotherapy [5]. However, only a minority of patients benefit and the response rate to anti-PD-1 mAb therapy in R/M HNSCC is only 15–20% [6]. There continues to be a great need for better predictive biomarkers for anti-PD-1 mAb therapy, including, ideally, noninvasive biomarkers from the peripheral blood that are not only predictive of response or prognosis but may also be a target for therapeutic intervention.

Recently, extracellular vesicles have emerged as potentially promising predictive biomarkers in cancer [7]. All cells can produce and release extracellular vesicles, including small (30–150 nm) extracellular vesicles (sEV) also known as exosomes. The sEV differ from other vesicles secreted by normal and malignant cells by biogenesis, small size and molecular contents [8]. They originate from the endocytic compartment of parent cells and carry a diverse cargo of receptors, enzymes, ligands and nucleic acids that reflects the cytosolic content and cell-surface molecules of the parent cells [7–9]. sEV serve as an intercellular communication system, delivering their cargo to near or distantly located cells and significantly altering the phenotype and functions of the recipient cells [10, 11]. This process, referred to as sEV-induced reprogramming, can have stimulatory or inhibitory effects on cells of the immune system [12]. Tumors take advantage of this communication system and use it to suppress the host anti-tumor immune responses [13]. In patients with cancer, tumor cells produce an excess of tumor-derived sEV or TEX, which carry various immunosuppressive proteins and reprogram functions of immune cells, leading to suppression of anti-tumor immunity [14–16]. TEX

[1]UPMC Hillman Cancer Center, Pittsburgh, PA, USA. [2]Department of Pathology, University of Pittsburgh School of Medicine, Pittsburgh, PA, USA. [3]Department of Human Genetics, School of Public Health, University of Pittsburgh, Pittsburgh, PA, USA. [4]Departments of Immunology and Otolaryngology, University of Pittsburgh School of Medicine, Pittsburgh, PA, USA. ✉email: diergaardeb@upmc.edu; whitesidetl@upmc.edu

Received: 7 June 2024 Revised: 12 August 2024 Accepted: 28 August 2024
Published online: 11 September 2024

interacting with activated T cells have been shown to induce de novo production and release of T cell-derived sEV capable of mediating immune suppression and promoting cancer progression [17].

Immune suppression driven by circulating TEX is a characteristic feature of HNSCC patients, and it has been associated with more advanced disease, nodal involvement, and cancer progression [18, 19]. Based on the potential role of these sEV in response of HNSCC patients to therapy, we hypothesized that also the response of HNSCC patients to immune checkpoint inhibition (ICI) might be influenced by circulating immunosuppressive sEV. In this study, we isolated sEV from pre-treatment plasma obtained from R/M HNSCC patients undergoing therapy with anti-PD-1 mAbs and evaluated their immunosuppressive profiles. Leveraging our capability to isolate fractions of TEX-enriched CD3(−) sEV as well as T cell-derived CD3(+) sEV from plasma, we aimed to evaluate the utility of sEV produced by the tumor, i.e., TEX, and of sEV produced by T cells as biomarkers of response to immunotherapy. We report that subsets of the sEV enriched in TEX and of the T cell-derived sEV may serve as prognostic biomarkers in anti-PD-1 mAb therapy treated R/M HNSCC. High plasma levels of the T cell-derived CD3(+) sEV and high levels of stimulatory and suppressive proteins on TEX-enriched CD3(−) sEV were associated with better patient outcomes.

METHODS

Study population

Patients with R/M HNSCC who received anti-PD-1 mAb therapy and had blood drawn prior to the start of immunotherapy (within 1 month before the first immunotherapy treatment) were included in this retrospective study, $N = 24$. The collection of blood samples and access to clinical data for research were reviewed and approved by the Institutional Review Board (IRB) of the University of Pittsburgh (IRB #: STUDY20030085). Clinical data obtained included baseline demographic and clinical characteristics as well as response by RECIST 1.1 criteria, and information on progression free survival (PFS) and overall survival (OS). Response was characterized as complete response (CR), partial response (PR), stable disease (SD) or progressive disease (PD). Disease control was defined as having CR, PR or SD. The patients' blood samples were delivered to the laboratory and centrifuged at 1000 × g for 10 min. Additionally, peripheral blood samples collected from five healthy donors (HDs) under the same IRB approved protocol were similarly processed. Plasma specimens were stored in 1 mL aliquots at −80 °C and were thawed immediately prior to sEV isolation.

Isolation of sEV from plasma

Thawed plasma samples were pre-cleared by two centrifugations at 2000 × *g* for 10 min then by 30 min centrifugation at 10,000 × *g* at 4 °C to sediment microvesicles (MVs). Supernatants were collected and ultrafiltered using 0.22 µm bacterial filters (EMD, Millipore). An aliquot (1 mL) of plasma was loaded onto a size exclusion chromatography (SEC) column (10 cm ×1 cm) packed with Sepharose 2B. A side-by-side row of 10 SEC columns were set up, and each patient's plasma sample was applied onto column and eluted with PBS. Eluate was collected in 1 mL fractions. sEV were eluted in the void volume, and fraction #4 containing the bulk of non-aggregated, morphologically intact sEV was harvested [20]. Isolated sEV were concentrated using Amicon Ultracel centrifugal concentrators (UCF510096, 100,000 MWCO).

sEV characterization

The vesicle size and particle numbers were determined using NanoSight 300 (Malvern, UK). The vesicles were diluted in ddH2O and then the video image was captured at the camera level of 14. The captured videos were analyzed using NTA software, maintaining the screen gain and the detection threshold at 1 and 5, respectively. To determine mean particle size/concentration in each sample, five consecutive measurements were obtained and averaged.

sEV transmission electron microscopy (TEM)

EVs were placed on copper grids coated with 0.125% formvar in chloroform and stained with a 1% uranyl acetate solution in ddH2O. Vesicles were visualized using TEM (model JEOL JEM-1011) as previously described [20].

Evaluation of sEV protein profiles by Western blot

Vesicle aliquots (10 µg protein) were lysed with Laemmli sample buffer (Bio-Rad Laboratories, Hercules, CA, USA), separated using 4–15% SDS/PAGE gels, and after transfer from gels to the polyvinylidene fluoride (PVDF) membranes, proteins were detected using Abs specific for antigens carried by sEV (see Supplementary Fig. 1) as previously described [21].

Determination of the protein content. The protein content in fraction #4 was determined using the BCA protein assay (Pierce Biotechnology, Rockford, CA) as per manufacturer's instructions.

Capture of total plasma sEV and CD3(+) sEV on magnetic beads. Total plasma sEV in fraction #4 were captured on ExoCap™ Streptavidin magnetic beads (MBL International, Woburn, MA). A 100 uL aliquot of the beads was co-incubated with the biotinylated anti-CD3 mAb (2 ug, clone Hit3a, Biolegend, San Diego, CA) or a mixture of biotinylated anti-CD63/CD81/CD9 mAbs (1 ug each, clones H5C6, TAPA-1, HI9a, respectively, Biolegend) for 2 h at room temperature (RT). For capture of total sEV on beads, sEVs (10 ug) were co-incubated with beads coated with a mix of biotinylated anti-CD63/CD81/CD9 mAbs (20 uL) for 12 h at 4 °C. For capture of CD3(+) vesicles, sEV (10 ug) were co-incubated with beads coated with anti-CD3 mAbs (20 uL). The uncaptured CD3(−) sEV were separated using a magnet and placed in new tubes. The captured CD3(+) sEV on beads were washed with buffer and used for the antigen detection by on-bead flow cytometry as described below. The CD3(−) sEV were re-captured with anti-CD63/CD81/CD9 beads. The reproducibility of the capture method for separation of CD3(+) sEV was tested by utilizing sEV from plasma of 3 different HNSCC patients and tested in three parallel assays for percentages of CD3(+) and CD3(−) sEV to determine experimental error as previously described [22].

Flow cytometry for detection of surface proteins on sEV

For the flow cytometry-based detection of antigens carried by sEV captured on beads, the method previously described by us [23] was used. Briefly, sEV on beads were dispensed into Eppendorf tubes and a fluorochrome-labeled detection Ab of choice was added to each tube. The beads were incubated with Abs for 30 min at RT on a shaker, washed 3x with PBS using a magnet and were re-suspended in 300 uL of PBS for antigen detection by flow cytometry. The following Abs were used for antigen detection: CD81APC (clone 1D6), CD3 PE (12–0037-42), CD14 PE (61D3), PD-1 PE (12-2799-42), PD-L1 PE (12–5983-42), FasL PE (NOK-1), TGFb LAP PE(12-9829-42), TRAIL PE (RIK-2), CTLA4 PE(14D3), CD40 PE (5C3), CD40L PE (24-31), OX40 PE (ACT-35), CD80 PE (2D10.4), TCRa/b PE (12-9955-42) all purchased from eBioscience. Additionally, CD44v3 APC (FAB5088A) from R&D Systems: OX40L PE (11C3.1) from Biolegend; and CD15s PE (563527) from BD Biosciences were used. Labeled isotype control Abs recommended by each vendor were used in all cases.

Titrations of Abs for flow cytometry-based detection

In preliminary titration experiments, different concentrations of the fluorochrome-conjugated detection Abs and isotype control Abs were used to determine the optimal conditions for staining and detection of the antigens of interest. The isotype control was used in all cases at the same concentration as the test Ab. The Ab concentration that gave the highest separation index (SI) between the detection Ab and the isotype control was selected for all experiments based on the formula: SI = (MFI labeled − MFI Isotype) /√((SD labeled^2 + SDIsotype^2)/2) [23].

Flow cytometry

Antigen detection on sEV was performed immediately after staining using LSR Fortessa flow cytometer (BD Biosciences, San Jose, CA, USA), and results were analyzed using Kaluza 2.1 software (Beckman Coulter, Krefeld, Germany). Samples were run for 2 min and around 10,000 events were acquired. Gates were set on the bead fraction visible in the forward/side light scatter. When sEVs obtained from plasma of HNSCC patients were analyzed by flow cytometry, the lower edge of the 'positive' gate was set so that 2% of the isotype control was included in this gate (2 standard deviations from the mean of isotype). Since this method detects sEVs bound on beads, the data are presented as Relative Fluorescence Values (RFV = MFI of stained sample/MFI of isotype control). However, to be able

to estimate total exosome protein (TEP) levels in the two sEV fractions separated by immune capture, we converted RFVs into percentages of positive sEV-bead complexes. The percentages closely reflect the RFVs, although they are not identical to these values.

Statistical analysis

Wilcoxon–Mann–Whitney tests were used to compare continuous variables between subject groups (e.g., patients *vs*. HDs); Wilcoxon signed-rank test was used when samples were not independent. Pearson correlation coefficients were calculated to examine whether continuous variables, e.g., the analyzed stimulatory proteins carried by CD3(−) sEV, correlated with each other. A stimulatory score was created by summing the RFVs for CD40, CD40L, OX40, OX40L, and CD80. Similarly, a suppressive score was created by summing the RFVs for TGFβ, CTLA-4, FASL, PD-L1, PD-1. In addition, we calculated the ratio of the suppressive and stimulatory scores (supp/stim ratio). The different stimulatory and suppressive proteins carried by CD3(−) sEV were also evaluated individually. Kaplan–Meier curves were estimated for OS and PFS; curves were compared using log-rank tests. The reverse Kaplan–Meier method was used to estimate the median follow-up time. Multivariable Cox proportional hazards models were used to assess the relationship between variables of interest (including TEP level, levels of specific sEV subsets, etc.) and OS and PFS; hazard ratios (HRs) and corresponding 95% confidence intervals (CIs) were calculated. Continuous variables were categorized for this as high/low based on the median, and the "low" category was used as the reference category throughout. P values < 0.05 were considered significant. Statistical analyses were performed using SAS® (version 9.4, SAS Institute Inc., Cary, NC, USA).

RESULTS

We identified 24R/M HNSCC patients treated with anti-PD-1 mAb whose plasma was obtained within one month prior to the start of their immunotherapy treatment, including 18 patients whose blood was drawn on the start day. All were included in this retrospective study. Selected baseline characteristics of the patients are shown in Table 1. Mean age was 62.4 years, and the majority of the patients was white, male and ever smoker. Oropharynx was the most common primary site (45.8%), and 81.8% of these tumors were HPV(+). Other primary sites included hypopharynx (16.7%), oral cavity (16.7%), and larynx (12.5%). Most of the patients had either local regional and/or distant recurrence, four patients (16.7%) had metastatic disease at diagnosis. Eleven (45.8%) patients received anti-PD-1 mAb therapy after failure of platinum-based chemotherapy, all other patients received anti-PD-1 for their frontline treatment of R/M disease. In our study population, the majority (54.2%) had PD as best response, with 16.7% and 29.1% achieving a PR and SD, respectively, and none of the patients a CR. Median follow-up time was 28.9 months (95% CI: 19.4- could not be estimated); 17 (70.8%) of the patients died and 20 (83.3%) progressed during follow-up. Median PFS was 5.3 months (95% CI: 1.6–8.1); median OS was 16.2 months (95% CI: 9.4–24.4).

Absolute lymphocyte counts of the patients were low at $1.0 \pm 1.2 \times 10^3$/uL (mean ± sd) and absolute neutrophil counts were elevated at $5.9 \pm 3.7 \times 10^3$/uL (mean ± sd) with a mean neutrophil-to-lymphocyte ratio (NLR) of 9.6 ± 7.3 (±sd) (Table 1). The NLR was significantly lower in patients who had PR or SD relative to patients with PD (6.0 ± 3.3 *vs*. 12.5 ± 8.4, $P = 0.02$); no significant differences were observed for absolute lymphocyte count and absolute neutrophil count (Fig. 1). The absolute lymphocyte and neutrophil counts did not correlate with total CD3(+) sEV or CD3(−) sEV recovered from the patients' plasma by immune capture (data not shown).

Total exosome protein (TEP) in sEV recovered from patients' plasma

Mean TEP levels were significantly higher in patients than in HDs (63.0 ± 33.7 ug/mL *vs*. 36.4 ± 13.2 ug/ml, $P = 0.04$; Fig. 2). There was no significant difference in TEP levels between patients with

Table 1. Selected characteristics of the study population ($N = 24$)

	***N* (%)**
Age at immunotherapy initiation in yrs	
mean (±sd)	62.4 (±9.8)
range	(44.4–81.3)
Sex, female	1 (4.2)
Race	
White	22 (91.7)
Black/African American	2 (8.3)
Ever smoker	
Yes	17 (70.8)
No	7 (29.2)
Primary[a]	
Oropharynx	11 (45.8)
Hypopharynx	4 (16.7)
Larynx	3 (12.5)
Oral cavity	4 (16.7)
Other[b]	2 (8.3)
HPV status[c]	
Positive	9 (37.5)
Negative	6 (25.0)
Not evaluated	9 (37.5)
Type of recurrence	
Local regional	6 (25.0)
Local regional plus distant	6 (25.0)
Distant	8 (33.3)
Metastatic at diagnosis	4 (16.7)
Type of immunotherapy received[d]	
Pembrolizumab	16 (66.7)
Other	8 (33.3)
Previous platinum failure, yes	11 (45.8)
Absolute neutrophil count in $\times 10^3$/uL	
mean (±sd)	5.9 (±3.7)
range	(1.6–17.3)
Absolute lymphocyte count in $\times 10^3$/uL	
mean (±sd)	1.0 (±1.2)
range	(0.2–6.4)
Neutrophil-lymphocyte ratio	
mean (±sd)	9.6 (±7.3)
range	(1.0–34.6)
Best response	
Partial response (PR)	4 (16.7)
Stable disease (SD)	7 (29.1)
Progressive disease (PD)	13 (54.2)
Disease control (PR or SD)	11 (45.8)
Alive at last follow up	7 (29.2)

[a]Oropharynx: 2 base-of-tongue, 8 tonsil, 1 unspecified; Oral cavity: 1 floor-of-mouth, 2 tongue, 1 unspecified; Other: 1 nasopharynx, 1 paranasal sinus.
[b]Other is: nasopharynx (1), paranasal sinus (1).
[c]Based on p16 and HPV ISH; all 9 HPV(+) tumor were located in the oropharynx. The not evaluated tumors included: larynx (N = 2), oral cavity (N = 3), hypopharynx (N = 3) and nasopharynx (N = 1). These HNSCC subsites are commonly HPV(−).
[d]Other is: cemiplimab (1), nivolumab (7).

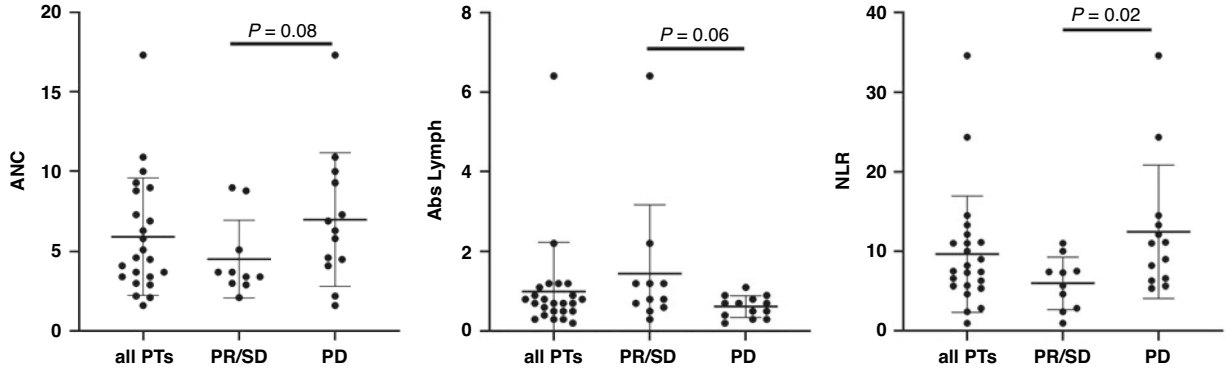

Fig. 1 Absolute neutrophil counts (×10^3/uL; ANC), absolute lymphocyte counts (×10^3/uL; Abs Lymp) and the neutrophil/lymphocyte (NRL) ratio in all patients (PTs) and in the patients stratified based on best response to immunotherapy. Wilcoxon–Mann–Whitney test was used to compare PR/SD with PD. PR partial response, SD stable disease; PD progressive disease. Each dot represents a subject. Mean with sd is shown. Note different scale of the y-axes.

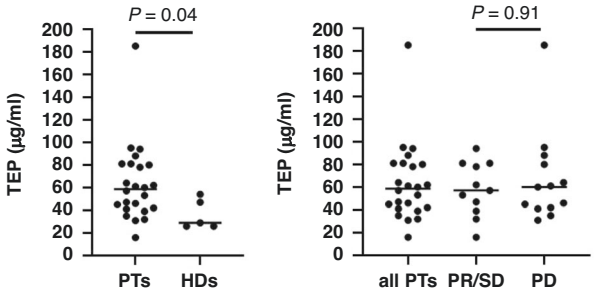

Fig. 2 TEP levels in HNSCC patients (PTs) and healthy donors (HDs) (*left panel*), and in the patients stratified based on best response to immunotherapy (*right panel*). Wilcoxon–Mann–Whitney test was used to compare the groups. PR partial response, SD stable disease, PD progressive disease. Each dot represents a subject. Horizontal bars indicate median TEP level.

HPV(+) *versus* those with HPV(−) tumors ($P = 0.51$) and no correlation between patient age and TEP level (Pearson correlation coefficient: 0.03, $P = 0.89$). In addition, TEP levels did not differ between patients with PR or SD and those with PD (58.2 ± 23.9 *vs.* 67.2 ± 40.8, $P = 0.91$), and TEP levels were also not associated with risk of disease progression and/or risk of death [low TEP level reference; HR: 1.84 (95% CI: 0.67–5.09), $P = 0.24$, and HR: 1.52 (95% CI: 0.49–4.77), $P = 0.47$, respectively; adjusted for: age at start immunotherapy, sex, race, HPV status (negative/not evaluated, positive), and smoking status (no, yes)].

Separation of total plasma sEV into CD3(+) and CD3(−) sEV subsets

Plasma-derived vesicles isolated using SEC were characterized for their protein content, morphology, size, presence of endocytic markers and absence of cytosol proteins as described in the Methods section and illustrated in Supplementary Fig. 1. According to the International Society for Extracellular Vesicles criteria [24], these vesicles are "small extracellular vesicles", sEV.

Total sEV isolated from patients' plasma were separated by immune capture into T cell-derived CD3(+) vesicles and CD3(−) vesicles derived from cells other than T cells, including tumor-cell derived sEV or TEX. Since there are no mAbs specific for a cell surface antigen exclusively expressed on HNSCC cells that can be used for immune capture of TEX, we used the mAb specific for the CD3 protein, a component of the TCR complex exclusively expressed on T cells, to capture CD3(+) sEV. Immune capture of sEV with anti-CD3 mAbs yielded two fractions: (a) the CD3(−) fraction largely composed of TEX plus various non-TEX (NTEX) derived from non-malignant immune or tissue cells, and (b) the CD3(+) fraction containing only CD3(+)/TCR(+) sEV derived from T cells (See Supplementary Fig. 2).

The efficacy of immunocapture was monitored by on-bead flow cytometry with anti-TCR mAbs for detection of CD3(+) T cell-derived sEV and with anti-CD44v3 mAbs for detection of CD44v3 protein, which is overexpressed on the surface of HNSCC cells and is detectable on sEV produced by these cells [25]. The representative RFI plots (Supplementary Fig. 3A, B) illustrate the results of immune capture in six patients. Supplementary Fig. 3A shows co-expression of TCR in CD3(+) sEV indicating that the vast majority of CD3(+) sEV are TCR(+), while CD3(−) sEV carry no/few TCR proteins on the vesicle surface. The CD3(−) fractions were variably enriched in CD44v3 protein, and expression levels of CD44v3 protein were higher in the CD3(−) *versus* the CD3(+) fractions (Supplementary Fig. 3B). The observed paucity of CD3(+) sEV among total sEV in the patients' plasma was not surprising given the observed low absolute lymphocyte counts (see above). The patients had few circulating T lymphocytes, which are the parent cells of CD3(+) sEV, as shown in Fig. 1.

Relative levels of CD3(+) and CD3(−) sEV from plasma of HNSCC patients

In total sEV specimens isolated from patients' plasma and prior to their separation by immune capture with anti-CD3 mAb, we evaluated the relative fluorescence values (RFVs) for TCR/CD3(+) sEV and CD3(−)CD44v3(+) sEV by on-bead flow cytometry. Figure 3 shows that the RFVs for these two sEV subsets varied significantly between the patients, and that the mean RFV for CD3(−)CD44v3(+) was significantly higher than the mean RFV for TCR/CD3(+) (6.8 ± 4.6 *vs.* 1.7 ± 0.7; $P < 0.0001$). These data indicate that the CD3(−)CD44v3(+) sEV fractions were much larger than the T cell derived CD3(+) sEV fractions in patients' plasma. This difference was independent of patient age and response to immunotherapy (data not shown). To further explore this result, we also calculated the relative TEP levels for each sEV fraction [TCR/CD3(+) and CD3(−)CD44v3(+)] from all patients and HDs by converting RFVs into percentages. As shown in SFigure 4, the mean relative TEP level in the CD3(+) sEV fraction was significantly lower in patients than in HDs (21% *vs.* 35% of total plasma TEP; $P = 0.04$). In contrast, the mean relative TEP level in the CD3(−) CD44v3(+) sEV fraction was significantly higher in patients than in HDs (67% *vs.* 15% of total plasma TEP; $P = 0.006$). In aggregate, we determined that the plasma from patients contained relatively few CD3(+) sEV, and that CD3(−)CD44v3(+) sEV represented the large majority of total plasma sEV.

We observed no significant association between CD3(−) CD44v3(+) sEV levels (categorized as high or low based on the median) and OS or PFS [HR: 0.30, 95% CI: 0.07–1.33, $P = 0.11$ and

HR: 0.99, 95% CI: 0.32–3.10, $P = 0.99$, respectively. Adjusted for age at start immunotherapy, sex, race, HPV status (negative/not evaluated, positive), smoking status (no, yes)] (Fig. 4a). There was also no significant difference in CD3(−)CD44v3(+) sEV levels between patients with PR or SD and those with PD ($P = 0.25$). The TCR/CD3(+) sEV levels also did not differ by best response ($P = 0.75$). Importantly, however, high TCR/CD3(+) sEV levels in patients' plasma were associated with significantly lower risk of death (OS) and lower risk of disease progression (PFS) compared to low TCR/CD3(+) sEV levels [HR: 0.16, 95% CI: 0.04–0.59, $P = 0.007$ and HR: 0.16, 95% CI: 0.04–0.58, $P = 0.005$, respectively; adjusted for age at start immunotherapy, sex, race, HPV status (negative/not evaluated, positive), smoking status (no, yes); Fig. 4b].

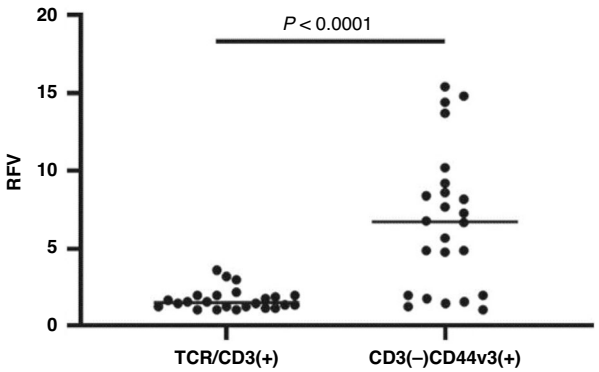

Fig. 3 Quantitation of TCR/CD3(+) and CD3(−)CD44v3(+) sEV fractions from all 24 patients by on-bead flow cytometry. Wilcoxon signed-rank test was used to compare the fractions. Each dot represents a subject. Horizontal bars indicate median RFV level. RFV relative fluorescence values.

Phenotypic analysis of CD3(−) sEV

Because of the paucity of CD3(+) sEV in the plasma from patients, we were only able to examine phenotypic characteristics of the CD3(−) sEV fractions by on-bead flow cytometry. We analyzed the stimulatory (CD40, CD40L, OX40, OX40L, CD80) and suppressive (TGFβ, CTLA-4, FASL, PD-L1, PD-1) proteins carried by the TEX-enriched CD3(−) sEV with the protein distributions illustrated in Supplementary Fig. 5. The data indicate broadly variable expression levels of suppressive and stimulatory proteins on CD3(−) sEV, except for CTLA-4 and CD40, which were overall low. Expression levels of PDL-1, PD-1, CD40L, OX40 and OX40L were highly elevated in sEV of some patients. Pearson correlation coefficients (Supplementary Table 1) for the evaluated surface markers of CD3(−) sEV indicated that CD80 expression level significantly correlated with all other co-stimulatory markers. Among inhibitory proteins, FasL, PDL-1 and TGFβ expression levels were correlated at $P = 0.0001$.

As described in the Methods section, we calculated stimulatory (stim) and suppressive (supp) scores for the CD3(−) sEV of each patient by adding up the RFVs of the individual stimulatory

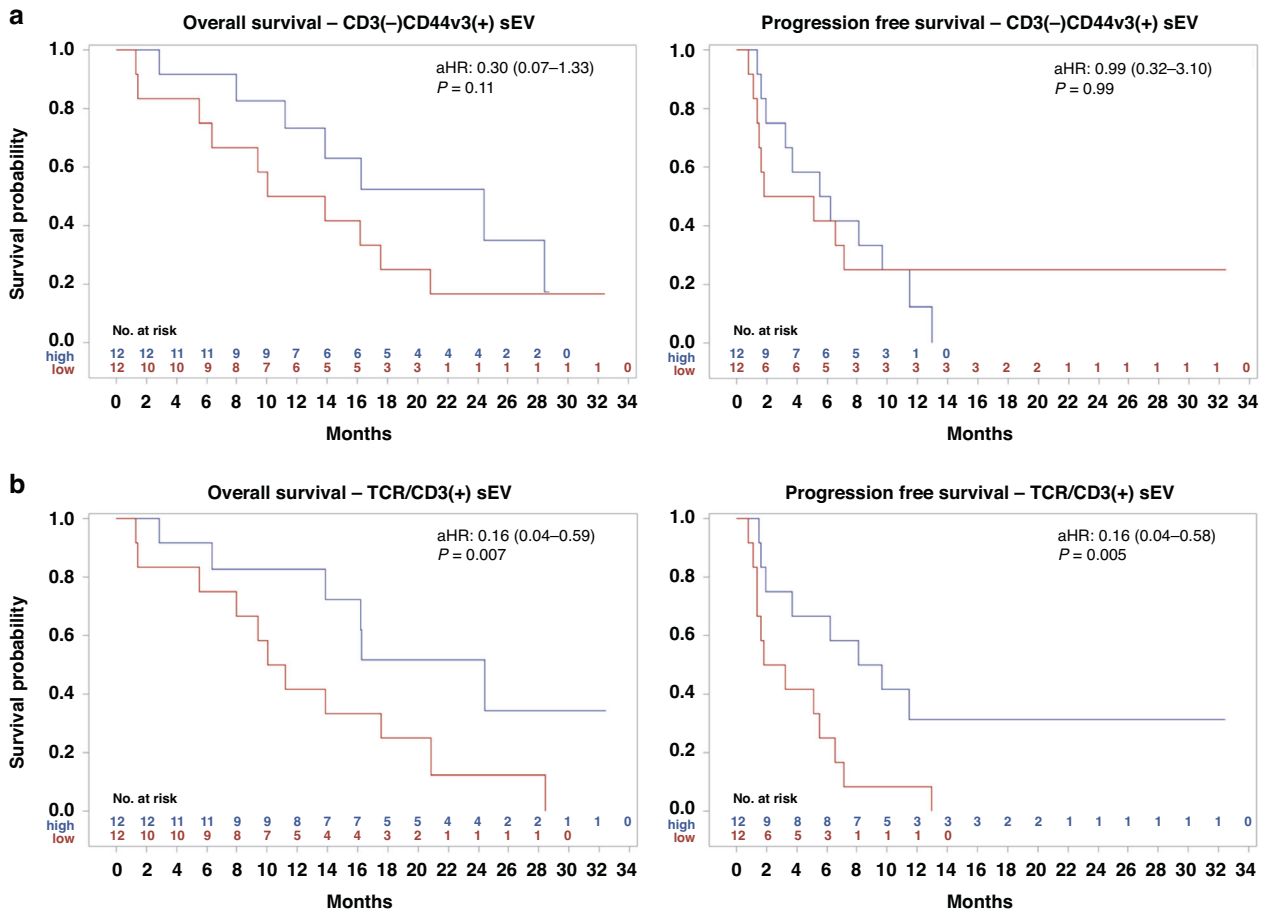

Fig. 4 CD3(−)CD44v3(+) sEV and TCR/CD3(+) sEV levels and patient outcomes. Kaplan–Meier overall survival (OS) and progression free survival (PFS) estimates by CD3(−)CD44v3(+) sEV (**a**) and TCR/CD3(+) sEV (**b**) category (high/low based on the median). The reference group is "low", adjusted hazard ratios (aHRs), corresponding 95% confidence intervals and *P* values are shown. Variables included in the Cox proportional hazards model: age at start immunotherapy, sex, race, HPV status (negative/not evaluated, positive), and smoking status (no, yes).

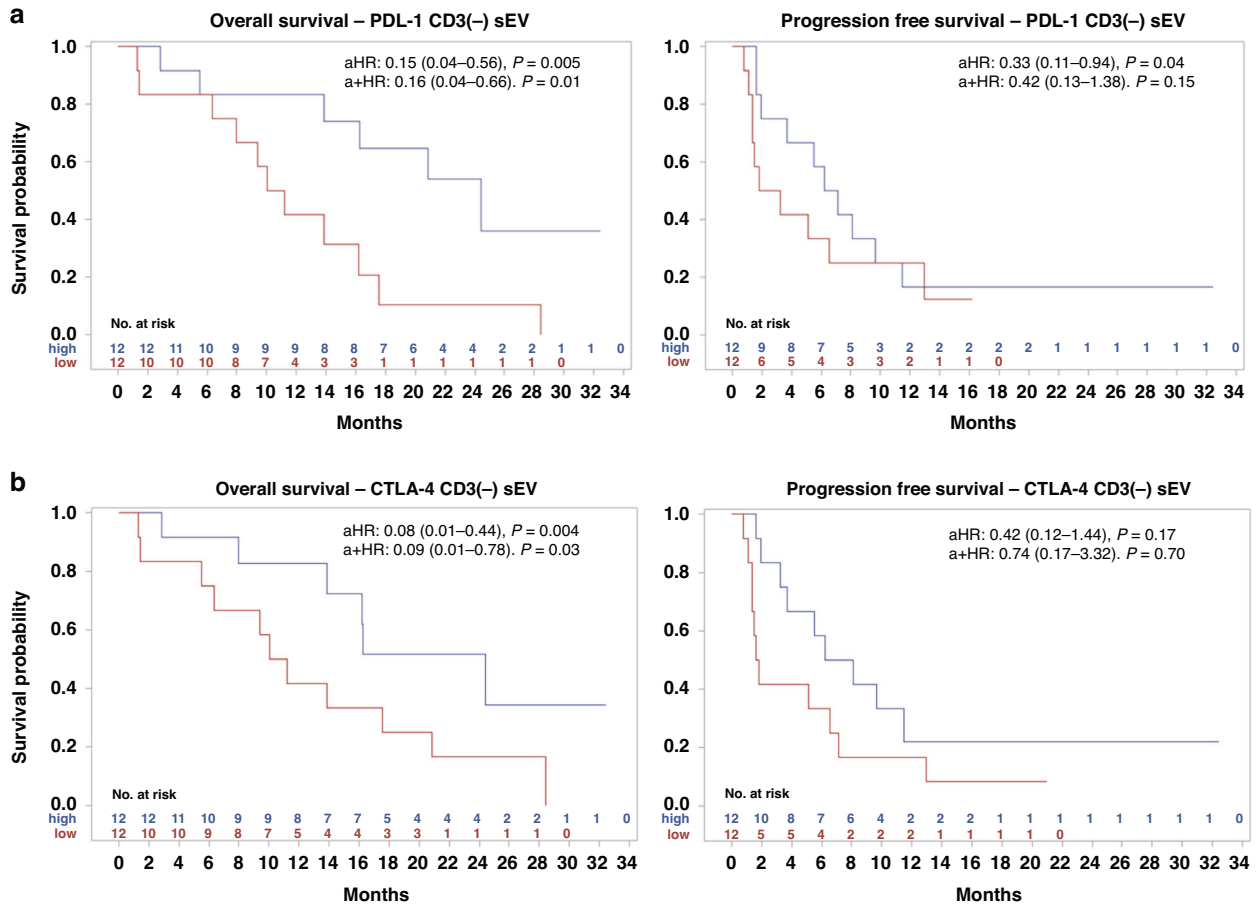

Fig. 5 Levels of PD-L1 and CTLA-4 on TEX-enriched CD3(−) sEV and patient outcomes. Kaplan–Meier overall survival (OS) and progression free survival (PFS) estimates by PD-L1 (**a**) and CTLA-4 (**b**) on TEX-enriched CD3(−) sEV category (high/low based on the median). The reference group is "low", adjusted hazard ratios (aHRs), corresponding 95% confidence intervals and *P* values are shown. Variables included in the Cox proportional hazards model: age at start immunotherapy, sex, race, HPV status (negative/not evaluated, positive), and smoking status (no, yes). Additional adjustment with PD-1 (low, high) for PD-L1 and with PD-L1 (low, high) for CTLA-4 is indicated as a+HR.

proteins or suppressive proteins. We observed no significant difference in the supp and stim scores of CD3(−) sEV between patients with PR or SD and those with PD ($P = 0.64$ and $P = 0.27$, respectively) (SFigure 6). However, the ratio of the supp and stim scores (supp/stim ratio), was significantly higher for patients with PR or SD than for those with PD ($P = 0.02$) (Supplementary Fig. 6). We also evaluated the relationship between the supp and stim scores of CD3(−) sEV and OS and PFS, with the scores categorized as high or low based on the median. Having a high supp score and having a high stim score were both associated with a significantly lower risk of death [supp score HR: 0.19, 95% CI: 0.05–0.77, $P = 0.02$ and stim score HR: 0.26, 95% CI: 0.07–0.95, $P = 0.04$; adjusted for age at start immunotherapy, sex, race, HPV status (negative/not evaluated, positive), smoking status (no, yes); Supplementary Fig. 7]. High supp score was also associated with a significantly lower risk of progression. We observed no significant association between supp/stim ratio categories and OS or PFS (Supplementary Fig. 7).

We next explored relationships between individual suppressive and stimulatory protein expression levels and outcomes (best response, OS and PFS). None of the suppressive markers (TGFβ, CTLA-4, FasL, PDL-1, and PD-1) or the stimulatory markers (CD40, CD40L, OX40, OX40L, and CD80) was individually significantly different between patients with PR or SD and those with PD (data not shown). High PD-L1 on TEX-enriched CD3(−) sEV was significantly associated with better OS (HR: 0.15, 95% CI: 0.04–0.56, $P = 0.005$), and PFS (HR: 0.33, 95% CI: 0.11–0.94, $P = 0.04$) [adjusted for age at start immunotherapy, sex, race, HPV status (negative/not evaluated, positive), smoking status (no, yes), Fig. 5a]. The relationship with OS remained significant after additional adjustment for PD-1, but not with PFS (OS HR: 0.16, 95% CI: 0.04–0.66, $P = 0.01$; PFS HR: 0.42, 95% CI: 0.13–1.38, $P = 0.15$). High CTLA-4 was significantly associated with better OS but not PFS (OS HR: 0.08, 95% CI: 0.01–0.44, $P = 0.004$; PFS HR: 0.42, 95% CI: 0.12–1.44, $P = 0.17$), the relationship with OS remained significant after additional adjustment for PD-L1 (HR: 0.09, 95% CI: 0.01–0.78, $P = 0.03$; Fig. 5b). None of the other proteins were individually significantly associated with OS or PFS independently of PD-L1 (data not shown).

DISCUSSION

In patients with advanced cancer, including R/M HNSCC, numbers of circulating sEV are elevated [26]. These sEV are heterogenous in their cellular origin, size and functions. We and others have previously shown that circulating tumor-derived vesicles (TEX) are molecular/genetic mimics of parent tumor cells and, thus, can serve as "liquid tumor biopsy" [27], while T cell derived CD3(+) sEV may be considered a "T cell biopsy" [28]. As such, both types of sEV could potentially be of use as noninvasive cancer biomarkers with diagnostic, prognostic and predictive significance.

Isolation from body fluids and separation of circulating sEV into distinct subsets provides means for determining their abundance and molecular/functional profiles, both of which are expected to

reflect the presence, activity and progression/regression of disease. Here, sEV isolated from plasma of patients with R/M HNSCC that was collected just prior to initiation of immunotherapy were separated by immune capture with anti-CD3 Ab into the subsets of T cell derived CD3(+) vesicles and CD3(−) vesicles which are enriched in TEX. Not unexpectedly, the TEX-enriched CD3(−) vesicle subset was significantly more abundant ($P < 0.0001$) than the CD3(+) subset, reflecting the paucity of circulating T cells and the presence of tumor metastases in this cohort of patients with R/M disease. The high NLR in these patients suggests the presence of immune abnormalities that could potentially benefit from immunotherapy with anti-PD1 mAb. We found that in patients with PD after immunotherapy, the NLR was significantly higher ($P < 0.02$) at baseline relative to patients with PR or SD.

To ask whether sEV isolated from the patients' pre-immunotherapy plasma have utility as biomarkers of response to anti-PD-1 mAbs, we first assessed the relationship between levels of recovered T cell derived CD3(+) sEV and TEX-enriched CD3(−) sEV subsets with outcome. We observed no significant associations between CD3(−) sEV level and best response, OS or PFS. However, high CD3(+) sEV level in patients' plasma was significantly associated with longer OS and lower risk of disease progression likely explainable by a better immune competence of these patients.

Results from our previous studies suggested that expression levels of suppressive and stimulatory proteins on the surface of sEV determine their functional interactions with immune cells [25]. In this study, we were unable to link the phenotypic profiles of the CD3(−) sEV to their functional attributes, as we did not recover sufficient sEV from the 1 mL of available plasma to perform functional assays. Expression levels of the suppressive and stimulatory proteins carried by CD3(−) sEV varied broadly in the patients from low to highly elevated. Focusing on TGFβ, CTLA-4, FasL, PD-L1, PD-1 as representative suppressive proteins, and on CD40, CD40L, OX40, OX40L, CD80 as stimulatory proteins carried on the sEV surface, we calculated supp and stim scores for the CD3(−) sEV of every patient and found that these scores were not significantly associated with best response. Surprisingly, the supp score was higher than the stim score in only a small majority of the patients ($N = 13$, see Supplementary Fig. 6 right panel), and the supp/stim ratio in patients with PD was significantly lower than in patients with PR or SD after therapy. These results differ from the data we previously reported for TEX of patients with other cancers (melanoma, breast cancer) [15, 29], suggesting that in patients with R/M HNSCC disease packaging of suppressive/stimulatory proteins into sEV by parent cells may be altered resulting in a distinct sEV phenotype. Importantly, however, both high supp and stim scores of CD3(−) sEV were significantly associated with better OS, and high supp score of CD3(−) sEV was also associated with lower risk of disease progression. These results could be interpreted as an indication that high expression levels of various immunoregulatory proteins on sEV surface may be beneficial for better outcome when patients are treated with immunotherapy.

In fact, none of the evaluated proteins carried by CD3(−) sEV were individually associated with best response. However, high PD-L1 level was associated with improved OS and PFS, and high CTLA-4 level was associated with improved OS independently of PD-L1. PD-L1(+)sEV have been observed to promote tumor growth and are associated with more aggressive clinicopathologic features and worse prognosis in solid tumors including HNSCC [18, 30, 31]. The responsible mechanisms may be linked to sEV-mediated suppression of effector T cells and stimulation of regulatory T cells (T regs) [32]. The predictive value of sEV PD-L1 level in anti-PD-1 mAb treated patients has been previously investigated in melanoma by Chen et al. who evaluated total circulating sEV and reported that higher pretreatment levels of sEV PD-L1 were associated with lower efficacy, as measured by objective response rate, of anti-PD-1 mAb therapy [31]. Interestingly, they observed increased sEV PD-L1 levels among clinical responders within six weeks of therapy, and reported that a larger increase in sEV PD-L1 level was associated with better outcomes [31]. Our results (i.e., the association of higher PD-L1 expression levels on CD3(−) sEV prior to immunotherapy with improved OS and PFS) are in line with the observed benefit of immunotherapy in patients with PD-L1-positive tumors, and might reflect the greater efficacy of anti-PD1 mAb when the PDL1-PD1 pathway is upregulated, allowing for its effective blockade by the Ab. In such case, expression levels of PD1 on the CD3(+) sEV surface would also be expected to be elevated and have prognostic significance. Like PD-L1 expression levels in the tumor, PD-L1 as a single biomarker in sEV is unlikely to reflect patients' overall immune status and analysis of its receptor, PD-1, expression on CD3(+) sEV would add credence to its prognostic significance. PD-1 levels on CD3(−) sEV varied widely (SFigure 5) and were not predictive of outcome. However, we were unable to phenotype CD3(+) sEV as indicated above and, therefore, were unable to evaluate the potential role of PD1 on CD3(+) sEV in predicting outcome. Thus, in patients with R/M HNSCC, molecular mechanisms responsible for the potential impact of high PD-L1 expression levels on CD3(−) sEV and response to anti-PD1 mAb remain undefined. Currently, plasma sEV slowly emerge as potential biomarkers of cancer presence, progression and response to immunotherapy [14, 27, 30, 31, 33], and it appears that the clinically relevant sEV biomarker profiles might be contextual and strictly dependent on the cancer type and disease activity. It is, therefore encouraging that in this small study we have identified several sEV associated proteins with significant prognostic value in R/M HNSCC patients undergoing immune therapy.

Our study had several limitations. The study population consisted of only 24 patients, most of whom received previous chemoradiation/radiation therapy, and none achieved a CR. Although the majority of patients, $N = 18$, had their blood drawn the day off starting anti-PD-1 mAb therapy, we included patients who had blood drawn up to one month before treatment start. As sEV production is a dynamic process which can change over time, the timing of the pre-therapy blood draw may be critical for the most accurate evaluation. Additionally, we worked with a limited plasma volume (1 mL) and recovered a low overall quantity of T cell derived CD3(+) sEV, mainly due to low absolute lymphocyte counts of our patients. Thus, phenotypic studies were only performed with TEX-enriched CD3(−) sEV, and functional studies were not possible.

Despite the limitations, we demonstrated that in addition to CD3(−) sEV serving as potential tumor cell biopsy, T cell derived CD3(+) sEV can also serve as a prognostically informative vesicle subset in support of the concept of liquid T cell biopsy in the same plasma sample. Future studies of prospectively acquired pre-therapy plasma are necessary to confirm and validate the role of sEV as predictive biomarkers of response to immunotherapy in patients with R/M HNSCC. Importantly, with ongoing research into modulation of sEV subsets, they have the potential to be not only a predictive biomarker for immunotherapy, but also one that could be someday therapeutically targeted to improve outcomes for patients.

DATA AVAILABILITY

Data are available from the corresponding authors upon reasonable request.

REFERENCES

1. Siegel RL, Giaquinto AN, Jemal A. Cancer statistics, 2024. CA Cancer J Clin. 2024. https://doi.org/10.3322/caac.21820.
2. Johnson DE, Burtness B, Leemans CR, Lui VWY, Bauman JE, Grandis JR. Head and neck squamous cell carcinoma. Nat Rev Dis Primers. 2020;6:92. https://doi.org/10.1038/s41572-020-00224-3.
3. Burtness B, Harrington KJ, Greil R, Soulières D, Tahara M, de Castro G Jr, et al. Pembrolizumab alone or with chemotherapy versus cetuximab with

chemotherapy for recurrent or metastatic squamous cell carcinoma of the head and neck (KEYNOTE-048): a randomised, open-label, phase 3 study. Lancet. 2019;394:1915–28. https://doi.org/10.1016/s0140-6736(19)32591-7.
4. Cramer JD, Burtness B, Le QT, Ferris RL. The changing therapeutic landscape of head and neck cancer. Nat Rev Clin Oncol. 2019;16:669–83. https://doi.org/10.1038/s41571-019-0227-z.
5. Ferris RL, Licitra L. PD-1 immunotherapy for recurrent or metastatic HNSCC. Lancet. 2019;394:1882–4. https://doi.org/10.1016/S0140-6736(19)32539-5.
6. Ferris RL, Blumenschein G Jr, Fayette J, Guigay J, Colevas AD, Licitra L, et al. Nivolumab for Recurrent Squamous-Cell Carcinoma of the Head and Neck. N Engl J Med. 2016;375:1856–67. https://doi.org/10.1056/NEJMoa1602252.
7. Kalluri R, LeBleu VS. The biology, function, and biomedical applications of exosomes. Science. 2020;367. https://doi.org/10.1126/science.aau6977.
8. Abels ER, Breakefield XO. Introduction to Extracellular Vesicles: Biogenesis, RNA Cargo Selection, Content, Release, and Uptake. Cell Mol Neurobiol. 2016;36:301–12. https://doi.org/10.1007/s10571-016-0366-z.
9. Hurwitz SN, Rider MA, Bundy JL, Liu X, Singh RK, Meckes DG Jr. Proteomic profiling of NCI-60 extracellular vesicles uncovers common protein cargo and cancer type-specific biomarkers. Oncotarget. 2016;7:86999–7015. https://doi.org/10.18632/oncotarget.13569.
10. Ludwig N, Yerneni SS, Razzo BM, Whiteside TL. Exosomes from HNSCC Promote Angiogenesis through Reprogramming of Endothelial Cells. Mol Cancer Res. 2018;16:1798–808. https://doi.org/10.1158/1541-7786.MCR-18-0358.
11. Maas SLN, Breakefield XO, Weaver AM. Extracellular Vesicles: Unique Intercellular Delivery Vehicles. Trends Cell Biol. 2017;27:172–88. https://doi.org/10.1016/j.tcb.2016.11.003.
12. Buzas EI. The roles of extracellular vesicles in the immune system. Nat Rev Immunol. 2023;23:236–50. https://doi.org/10.1038/s41577-022-00763-8.
13. Whiteside TL. Exosomes and tumor-mediated immune suppression. J Clin Invest. 2016;126:1216–23. https://doi.org/10.1172/JCI81136.
14. Ludwig S, Floros T, Theodoraki MN, Hong CS, Jackson EK, Lang S, et al. Suppression of Lymphocyte Functions by Plasma Exosomes Correlates with Disease Activity in Patients with Head and Neck Cancer. Clin Cancer Res. 2017;23:4843–54. https://doi.org/10.1158/1078-0432.CCR-16-2819.
15. Sharma P, Diergaarde B, Ferrone S, Kirkwood JM, Whiteside TL. Melanoma cell-derived exosomes in plasma of melanoma patients suppress functions of immune effector cells. Sci Rep. 2020;10:92. https://doi.org/10.1038/s41598-019-56542-4.
16. Xie QH, Zheng JQ, Ding JY, Wu YF, Liu L, Yu ZL, et al. Exosome-Mediated Immunosuppression in Tumor Microenvironments. Cells. 2022;11. https://doi.org/10.3390/cells11121946.
17. Zebrowska A, Jelonek K, Mondal S, Gawin M, Mrowiec K, Widłak P, et al. Proteomic and Metabolomic Profiles of T Cell-Derived Exosomes Isolated from Human Plasma. Cells. 2022;11. https://doi.org/10.3390/cells11121965.
18. Theodoraki MN, Yerneni SS, Hoffmann TK, Gooding WE, Whiteside TL. Clinical Significance of PD-L1(+) Exosomes in Plasma of Head and Neck Cancer Patients. Clin Cancer Res. 2018;24:896–905. https://doi.org/10.1158/1078-0432.CCR-17-2664.
19. Theodoraki MN, Hoffmann TK, Jackson EK, Whiteside TL. Exosomes in HNSCC plasma as surrogate markers of tumour progression and immune competence. Clin Exp Immunol. 2018;194:67–78. https://doi.org/10.1111/cei.13157.
20. Hong CS, Funk S, Muller L, Boyiadzis M, Whiteside TL. Isolation of biologically active and morphologically intact exosomes from plasma of patients with cancer. J Extracell Vesicles. 2016;5:29289. https://doi.org/10.3402/jev.v5.29289
21. Ludwig N, Razzo BM, Yerneni SS, Whiteside TL. Optimization of cell culture conditions for exosome isolation using mini-size exclusion chromatography (mini-SEC). Exp Cell Res. 2019;378:149–57. https://doi.org/10.1016/j.yexcr.2019.03.014.
22. Sharma P, Ludwig S, Muller L, Hong CS, Kirkwood JM, Ferrone S, et al. Immunoaffinity-based isolation of melanoma cell-derived exosomes from plasma of patients with melanoma. J Extracell Vesicles. 2018;7:1435138. https://doi.org/10.1080/20013078.2018.1435138
23. Theodoraki MN, Hong CS, Donnenberg VS, Donnenberg AD, Whiteside TL. Evaluation of Exosome Proteins by on-Bead Flow Cytometry. Cytometry A. 2020. https://doi.org/10.1002/cyto.a.24193.
24. Thery C, Witwer KW, Aikawa E, Alcaraz MJ, Anderson JD, Andriantsitohaina R, et al. Minimal information for studies of extracellular vesicles 2018 (MISEV2018): a position statement of the International Society for Extracellular Vesicles and update of the MISEV2014 guidelines. J Extracell Vesicles. 2018;7:1535750. https://doi.org/10.1080/20013078.2018.1535750
25. Theodoraki M-N, Matsumoto A, Beccard I, Hoffmann TK, Whiteside TL. CD44v3 protein-carrying tumor-derived exosomes in HNSCC patients' plasma as potential noninvasive biomarkers of disease activity. OncoImmunology. 2020;9:1747732. https://doi.org/10.1080/2162402X.2020.1747732.
26. Cappello F, Fais S. Extracellular vesicles in cancer pros and cons: The importance of the evidence-based medicine. Semin Cancer Biol. 2022;86:4–12. https://doi.org/10.1016/j.semcancer.2022.01.011.
27. Pietrowska M, Zebrowska A, Gawin M, Marczak L, Sharma P, Mondal S, et al. Proteomic profile of melanoma cell-derived small extracellular vesicles in patients' plasma: a potential correlate of melanoma progression. J Extracell Vesicles. 2021;10:e12063. https://doi.org/10.1002/jev2.12063.
28. Theodoraki MN, Hoffmann TK, Whiteside TL. Separation of plasma-derived exosomes into CD3((+)) and CD3((−)) fractions allows for association of immune cell and tumour cell markers with disease activity in HNSCC patients. Clin Exp Immunol. 2018;192:271–83. https://doi.org/10.1111/cei.13113.
29. Mondal SK, Haas D, Han J, Whiteside TL. Small EV in plasma of triple negative breast cancer patients induce intrinsic apoptosis in activated T cells. Commun Biol. 2023;6:815. https://doi.org/10.1038/s42003-023-05169-3.
30. Xie F, Xu M, Lu J, Mao L, Wang S. The role of exosomal PD-L1 in tumor progression and immunotherapy. Mol Cancer. 2019;18:146. https://doi.org/10.1186/s12943-019-1074-3.
31. Chen G, Huang AC, Zhang W, Zhang G, Wu M, Xu W, et al. Exosomal PD-L1 contributes to immunosuppression and is associated with anti-PD-1 response. Nature. 2018;560:382–6. https://doi.org/10.1038/s41586-018-0392-8.
32. Szajnik M, Czystowska M, Szczepanski MJ, Mandapathil M, Whiteside TL. Tumor-derived microvesicles induce, expand and up-regulate biological activities of human regulatory T cells (Treg). PLoS One. 2010;5:e11469. https://doi.org/10.1371/journal.pone.0011469.
33. Hoshino A, Kim HS, Bojmar L, Gyan KE, Cioffi M, Hernandez J, et al. Extracellular Vesicle and Particle Biomarkers Define Multiple Human Cancers. Cell. 2020;182:1044–61.e18. https://doi.org/10.1016/j.cell.2020.07.009.

AUTHOR CONTRIBUTIONS

DPZ: Investigation, Resources, Data curation, Writing—original draft, Writing—reviewing and editing, Funding Acquisition. C-SH: Formal Analysis, Investigation, Visualization, Writing—reviewing and editing. AS, RH and JA: Data curation, Writing—reviewing and editing. RLF: Resources, Writing—reviewing and editing. BD: Methodology, Data curation, Formal Analysis, Investigation, Validation, Visualization, Writing—original draft, Writing—reviewing and editing, Funding Acquisition. TLW: Conceptualization, Methodology, Investigation, Validation, Resources, Supervision, Writing—original draft, Writing—reviewing and editing, Project Administration, Funding Acquisition.

FUNDING

This research was funded in part by NIH grants U01-DE029759, R01-DE031299, P50-CA097190 and P30-CA047904.

COMPETING INTERESTS

Competing interests: None for C-SH, AS, RH, JA, BD and TLW. DPZ: Steering Committee (BICARA, Seagen Inc.); Consulting (Inhibrx, MacroGenics Inc.); Advisory Board (Merck, Prelude Therapeutics); Research support (institutional) for role as PI for clinical trials with Aduro Biotech Inc., Astra-Zeneca, Bicara Therapeutics Inc., Bristol-Myers Squibb, GlaxoSmithKline, MacroGenics Inc., Merck, Novasenta. RLF: Adagene Incorporated: Consulting; Adaptimmune: H&N Cancer Advisory Board; Aduro Biotech, Inc: Consulting; Astra-Zeneca/MedImmune: Clinical Trial, Research Funding; Bicara Therapeutics, Inc: Consultant; Bristol-Myers Squibb: Advisory Board, Clinical Trial, Research Funding; Brooklyn Immunotherapeutics LLC: Consultant; Catenion: Consultant; Coherus BioSciences, Inc.: Advisory Board; CureVac : H&N Advisory Board; CytoAgents: Board; Eisai Europe Limited: Advisory Board; EMD Serono: Consultant; Everest Clinical Research Corporation: Consultant; F. Hoffmann-La Roche Ltd: Consultant; Federation Bio, Inc: Consultant; Genocea Biosciences, Inc: Consultant; Genmab: Advisory Board; Hookipa Biotech GmbH: Advisory Board; Instil Bio, Inc: Advisory Board; Kowa Research Institute, Inc.: Consultant; Lifescience Dynamics Limited: Advisory Board; MacroGenics, Inc.: Advisory Board; MeiraGTx, LLC: Advisory Board; Merck: Advisory Board, Clinical Trial; Merus N.V: Advisory Board; Mirati Therapeutics, Inc: Consultant; Mirror Biologics Inc: Data Safety Monitoring Board; Nanobiotix: Consultant; Novartis Pharmaceutical Corporation: Consulting; Novasenta: Consulting, Stock, Research Funding; Numab Therapeutics AG: Advisory Board; OncoCyte Corporation: Advisory Board; Pfizer: Advisory Board; PPD Development, L.P.: Consultant; Rakuten Medical, Inc: Advisory Board; Regeneron: H&N Advisory Board; Sanofi: Consultant; Seagen, Inc: Advisory Board; SIRPant Immunotherapeutics, Inc: Advisory Board; Tesaro: Research Funding; Vir Biotechnology, Inc: Advisory Board; Zymeworks, Inc.: Consultant.

ETHICS APPROVAL AND CONSENT TO PARTICIPATE

The study was approved by the Institutional Review Board of the University of Pittsburgh (IRB #: STUDY20030085). Written informed consent was obtained from all

study participants. The study was performed in accordance with the Declaration of Helsinki.

ADDITIONAL INFORMATION

Supplementary information The online version contains supplementary material available at https://doi.org/10.1038/s44276-024-00096-0.

Correspondence and requests for materials should be addressed to Brenda Diergaarde or Theresa L. Whiteside.